Polymer Degradation and Stability 94 (2009) 2042–2054

Contents lists available at ScienceDirect

Polymer Degradation and Stability

journal homepage: www.elsevier.com/locate/polydegstab

Polymer nanocomposites using zinc aluminum and magnesium aluminum oleate layered double hydroxides: Effects of the polymeric compatibilizer and of composition on the thermal and fire properties of PP/LDH nanocomposites

Charles Manzi-Nshuti [a], Ponusa Songtipya [b,c], Evangelos Manias [b], Maria del Mar Jimenez-Gasco [c], Jeanne M. Hossenlopp [a], Charles A. Wilkie [a,*]

[a] Department of Chemistry and Fire Retardant Research Facility, Marquette University, 535 N 14th Street, Milwaukee, WI 53201-1881, USA
[b] Polymer Nanostructures Lab – Center for the Study of Polymeric Systems, and Department of Materials Science & Engineering, Penn State University, University Park, PA, USA
[c] Plant Pathology Department, Penn State University, University Park, PA, USA

ARTICLE INFO

Article history:
Received 18 May 2009
Accepted 17 July 2009
Available online 24 July 2009

Keywords:
Nanocomposites
Layered double hydroxides
Polypropylene
Cone calorimetry

ABSTRACT

A series of five oleate-containing layered double hydroxides with varied ratios of zinc to magnesium, *i.e.*, with the general formula $Zn_{2-y}Mg_yAl(OH)_6$ $[CH_3(CH_2)_7CH{=}CH(CH_2)_7COO]\cdot nH_2O$, were synthesized and used to prepare nanocomposites of polypropylene (PP). The nanomaterials were characterized by elemental analysis, attenuated total reflection-infrared spectroscopy (ATR-IR), X-ray diffraction (XRD) and thermogravimetric analysis (TGA), while the composites were characterized by XRD, TGA, transmission electron microscopy (TEM) and cone calorimetry. The zinc-containing LDH showed better dispersion in the polymer at the micrometer level than did the magnesium-containing LDH while both are equally well-dispersed at the nanometer level. The magnesium-containing composites led to more thermally stable systems in TGA experiments, while the zinc systems gave greater reductions in heat release rate during combustion. Dispersion was also affected by the amount of PP-*g*-MA which was present. More PP-*g*-MA gave better dispersion and a significantly reduced peak heat release rate, *i.e.*, enhanced fire performance.

1. Introduction

Polymer nanocomposites have been extensively studied for a variety of applications including improved thermo-mechanical properties, gas barrier performance, improved thermal properties, and greatly reduced flammability [1,2]. Most of the published work has focused on organically modified smectite clays, in particular montmorillonites, as fillers of polymeric composites [2]. Recently, considerable interest for preparing, shaping, and improving solids to match the ever-growing demand for multifunctional materials has created a growing interest in other types of layered nanomaterials, like the layered double hydroxides (LDHs), commonly also called anionic clays [3].

LDHs find applications as catalysts, catalyst precursors, adsorbents, anion exchangers, thermal stabilizers, hosts for nanoscale reactions, and so on [4,5] The general formula of these layered double hydroxides, also known as hydrotalcite-like compounds, is $[M^{II}_{1-x}M^{III}_x(OH)_2]^{x+}A_{x/m}{}^{m-}\cdot nH_2O$, where M^{II} is a divalent cation, such as Mg, Co, Ni, Cu, or Zn; M^{III} is a trivalent cation, such as Al, Cr, Fe, V, or Ga; and A is an *m*-valent inorganic or organic anion [6]. The structure of the hydrotalcite is that of the brucite crystallographic layered structure, in which trivalent cations partially substitute for divalent cations and a commensurate number of anions are therefore incorporated between the layers to balance the charge.

Nanocomposite formation in polymer matrices can be accomplished by solution mixing, *in situ* polymerization, or melt mixing. With montmorillonite as the nano-dimensional material, solution and *in situ* polymerization typically yield better dispersions of the nanoparticles in the polymer matrix at the nanometer level, but the melt mixing approach is probably more appropriate for industrial or large scale use, since it employs current industrial compounding methods, and the absence of organic solvents renders this process more environmentally benign and economic [7]. Organically modified LDH layers have been dispersed in various polymers, such as poly(ethylene-*graft*-maleic anhydride) (PE-*g*-MA) [8], poly (methyl methacrylate) (PMMA) [9], linear low-density polyethylene (LLDPE) [10], polyimide (PI) [11], and polystyrene [12]. Because of their highly tunable properties, these nanocomposite materials are evaluated for potential application in a large number of fields, such as those emphasizing mechanical performance [13] and as polymer electrolytes [14,15].

* Corresponding author. Tel.: +1 414 288 7239; fax.: +1 414 288 7066.
E-mail address: charles.wilkie@marquette.edu (C.A. Wilkie).

0141-3910/$ – see front matter © 2009 Elsevier Ltd. All rights reserved.
doi:10.1016/j.polymdegradstab.2009.07.013

Recently, these LDH nanomaterials have also been investigated as potential fire retardant (FR) additives for polymers [16]. The advantages, but also the challenges, associated with using these LDHs as fire retardant additives for polymers, arise from the numerous compositions of LDH that can be prepared. In investigations of the flammability of PMMA, for example, it was found that the fire properties of LDH-reinforced composites depend on the type of both the divalent and trivalent metal cations, and also on the type and size of the intercalated anions [17–19], With this polymer, the best fire performances, more than 50% reduction in PHRR [20] relative to the pristine polymer, have been reported for melt blended PMMA modified with organically modified magnesium aluminum LDHs [21].

The current work investigates the use of LDH nanomaterials as additives for polypropylene (PP) systems prepared by melt blending. PP composites with the more common cationic clays, such as layered alumino-silicates, have proven that it remains rather difficult to obtain good dispersion at the nanometer scale. For example, montmorillonite (MMT) is not readily-miscible with non-polar polymers, such as PP, and the use of functionalized-PP intermediates (such as PP-*graft*-maleic anhydride, PP-*g*-MA) is needed to predisperse the nanofiller, before preparing PP/clay nanocomposites [22–26], Other more unusual approaches include the extrusion of unmodified PP with an edge-functionalized MMT bearing a semi-fluorinated organic modification [24], or the quiescent melt-intercalation of end-functionalized PP-*term*-ammonium in pristine Na^+ MMT [27], and "one step" preparation of PP/MMT nanocomposites by using pristine MMT, PP, PP-*g*-MA and long-alkyl ammonium surfactants [28–30].

In this study, a series of analogous Zn/Mg/Al-Oleate LDHs with various contents of zinc and magnesium were prepared and used to form nanocomposites with polypropylene (PP) by melt blending. The influence of LDH composition and of the presence of a polymeric compatibilizer, PP-*g*-MA, as well as dispersion and properties of PP/LDH system are investigated.

2. Experimental

2.1. Materials

Zinc nitrate hexahydrate (98%), magnesium nitrate hexahydrate (99%), aluminum nitrate nonahydrate (98%), and sodium hydroxide (extra-pure pellets) were purchased from Aldrich Chemical Co. Purified sodium oleate powder was obtained from J.T. Baker. Polypropylene (PP, Petrothene PP 31KK01) was provided by Equistar Chemicals and polypropylene maleic anhydride copolymer (PP-*g*-MA, Polybond X5104) was generously provided by Crompton.

2.2. Synthesis of LDHs

The theoretical compositions of the five LDHs prepared in this study are provided in Table 1. The synthesis of oleate-containing LDHs of zinc aluminum and magnesium aluminum has been fully described previously [31]. Similarly, ternary LDHs of Zn_xMg_yAl, were produced by replacing zinc nitrate with magnesium nitrate according to the ratios shown in Table 1. In all five LDHs, the ratio of the divalent cations to the trivalent cations is maintained at 2–1.

Table 1
LDH formulations and their ideal formulas based on the recipe followed.

Metal mole ratios				Ideal LDH formula
LDH code	Zn	Mg	Al	
AA	0.0	2.0	1.0	$Mg_{2.00}Al(OH)_{6.00}(C_{18}H_{33}O_2)\cdot nH_2O$
AB	0.5	1.5	1.0	$Zn_{0.50}\ Mg_{1.50}Al(OH)_{6.00}(C_{18}H_{33}O_2)\cdot nH_2O$
AC	1.0	1.0	1.0	$Zn_{1.00}\ Mg_{1.00}Al(OH)_{6.00}(C_{18}H_{33}O_2)\cdot nH_2O$
AD	1.5	0.5	1.0	$Zn_{1.50}\ Mg_{1.50}Al(OH)_{6.00}(C_{18}H_{33}O_2)\cdot nH_2O$
AE	2.0	0.0	1.0	$Zn_{2.00}\ Al(OH)_{6.00}(C_{18}H_{33}O_2)\cdot nH_2O$

The elemental analysis results obtained for AA, are as follows: 8.54% Mg, 4.51% Al, 45.18% C, 8.57% H, 0.02% N, 0.67% Na with atomic ratio Mg/Al = 2.10; the respective calculated values for AA are: 8.94% Mg, 4.72% Al, 44.95% C, 8.91% H, 0.00% N, 0.76% Na with the formula $Mg_{2.10}Al(OH)_{6.20}\ (C_{18}H_{33}O_2)\ (C_{18}H_{33}O_2Na)_{0.19}\ 2.75H_2O$. Experimental for AB, 8.05% Zn, 5.67% Mg, 4.46% Al, 43.00% C, 8.31% H, 0.02% N, 0.39% Na with atomic ratio (Zn + Mg)/Al = 2.16; and calculated for AB: 8.19% Zn, 5.76% Mg, 4.53% Al, 42.97% C, 8.39% H, 0.00% N, 0.71% Na corresponding to the formula $Zn_{0.75}Mg_{1.41}Al(OH)_{6.31}(C_{18}H_{33}O_2)\ (C_{18}H_{33}O_2Na)_{0.18}\ 2.27H_2O$. Experimental for AC: 12.25% Zn, 4.32% Mg, 4.30% Al, 43.51% C, 8.37% H, 0.03% N, 0.31% Na with atomic ratio (Zn + Mg)/Al = 2.30; and calculated for AC: 12.03% Zn, 4.24% Mg, 4.22% Al, 43.11% C, 8.16% H, 0.00% N, 0.99% Na suggesting the formula $Zn_{1.18}Mg_{1.12}Al(OH)_{6.58}\ (C_{18}H_{33}O_2)\ (C_{18}H_{33}O_2Na)_{0.28}\ 1.74H_2O$. Experimental for AD: 15.54% Zn, 2.72% Mg, 4.19% Al, 42.09% C, 0.02% N, 8.06% H, 0.17% Na with the atomic ratio (Zn + Mg)/Al = 2.25; and calculated for AD: 15.48% Zn, 2.71% Mg, 4.17% Al, 42.04% C, 0.00% N, 7.98% H, 0.91% Na corresponding to the formula $Zn_{1.53}Mg_{0.72}Al(OH)_{6.50}\ (C_{18}H_{33}O_2)\ (C_{18}H_{33}O_2Na)_{0.26}\ 1.76H_2O$. Experimental for AE: 23.54% Zn, 3.88% Al, 39.87% C, 7.45% H, 0.02% N, 0.64% Na with the atomic ratio Zn/Al = 2.49; and calculated for AE: 23.44% Zn, 3.88% Al, 39.91% C, 7.40% H, 0.00% N, 0.94% Na corresponding to the formula $Zn_{2.49}Al(OH)_{6.98}(C_{18}H_{33}O_2)\ (C_{18}H_{33}O_2Na)_{0.28}\ 1.05H_2O$.

2.3. Preparation of (nano)composites

The (nano)composites were prepared in a Brabender Plasticorder twin-head kneader at high speed (60 rpm) at 180 °C. The residence time in the Brabender mixer was 10 min for all composites. The composition of each nanocomposite is calculated from the amounts of layered double hydroxide (wt.%) and polymer charged to the Brabender.

2.4. Instrumentation

Attenuated total reflection-infrared (FTIR) spectroscopy of the solid materials were obtained on a Bruker Tensor 27 series, with a Pike Miracle ATR accessory using a ZnSe crystal. Elemental analysis was carried out by Huffman Labs, Colorado, using atomic emission spectroscopy interfaced with inductively coupled plasma (AES-ICP) for metal determination. Thermogravimetric analysis (TGA) was performed on an SDT 2960 instrument (TA instrument) at the 15 mg scale under a flowing air atmosphere at a scan rate of 20 °C/min. Temperatures are reproducible to ±3 °C, while the error on the fraction of non-volatile materials is ±2%. TGA was done in duplicate and the averages are reported. X-ray diffraction (XRD) measurements were performed on a Rigaku Miniflex II desktop X-ray diffractometer; data acquisition was performed using a scan speed of 2 °/min, at a sampling width of 0.020° from 2° to 40° (2θ) for LDHs, 2° to 10° (2θ) for composites, and 2° to 70° (2θ) for cone residues. Bright field transmission electron microscopy (TEM) was performed in a JEOL 1200 EXII microscope, equipped with a Tietz F224 digital camera, and operated at an accelerating voltage of 80 kV. Sections of the nanocomposites were obtained with a Leica Ultracut UCT microtome, equipped with a diamond knife. The sections were transferred to carbon-coated copper grids (200-mesh), with or without a carbon lace, and imaged without any heavy metal staining. Cone calorimeter measurements were performed on an Atlas CONE-2 according to ASTM E1352 at an incident flux of 50 kW/m^2, using a cone shaped heater; the exhaust flow was set at 24 l/s. The specimens for cone calorimetry were prepared by compression molding of the sample (about 30 g) into 3 × 100 × 100 mm^3 square plaques.

Typical results from cone calorimetry are reproducible to within about ±10%; these uncertainties are based on many runs in which thousands of samples have been combusted [32].

3. Results and discussion

A series of five oleate-containing LDHs were prepared in this work and their compositions are provided in Table 1. Oleate anions were used as the organic compatibilizer to have organophilic character in the LDH interlayer region. This anion is preferred to other possible surfactants because of its excellent combination of high thermal stability, good water solubility, and relatively low cost.

The preparation of two-metal LDHs is very common in the literature, and ternary (three-metal) LDHs have also been prepared and characterized before [33,34], The elemental analysis results provided in the experimental section reveal that the target metals, zinc and/or magnesium and aluminum, are present in the LDHs and that the metal content used in the syntheses correlates well with the content in the produced LDHs. The ratio of the divalent to trivalent metal cations for the five LDHs is in the range 2.10–2.49 and decreases gradually as the magnesium content in the LDH decreases (from AA to AE). A good correlation of divalent to trivalent metal cations in LDH produced by the coprecipitation method was also observed by Wang et al., who reported that the ratio of the divalent to the trivalent metal cations was maintained at 2:1 in both the reactants and the product (MgAl-undecenoate) LDH [35]. This observation was attributed to the fact that the solubility of the metal (II) hydroxide greatly exceeds that of the aluminum hydroxide [36].

The XRD patterns in the range of $2\theta = 2$–40° for the five oleate-containing LDHs prepared in this work are shown in Fig. 1. At least two diffraction peaks at equidistant 2θ values are observed for all five materials, an indication of a well-defined layered structure for these LDHs. The interlayer spacings, calculated using the Bragg equation, are in the range 3.5–3.7 nm. The relatively large interlayer spacings of these materials may be due to the unusual packing of the long oleate anions in the gallery of these LDHs [37].

3.1. IR characteristics of the oleate LDHs

Fig. 2 provides the IR spectra of the five oleate-containing LDHs along with the spectra of sodium oleate. These spectra confirm the presence of oleate anions in the LDH materials produced; the broad band at ~ 3500 cm^{-1} (ν-$_{OH}$ of hydroxide), the asymmetric and symmetric ν-$_{CH}$ at 3000–2800 cm^{-1}, and the two strong bands at 1600–1400 cm^{-1} (asymmetric and symmetric carboxylate bands). There is also another distinctive feature: a weak peak in the range 3005–3010 cm^{-1} associated with ν-$_{CH}$ attached to a double carbon–carbon bond [38].

3.2. Thermogravimetric analysis of the oleate LDHs

The TGA curves of oleate-containing LDHs, heated in air from 50 to 800 °C, show several stages of thermolysis (Fig. 3). The first stage (below 150 °C) is attributed to loss of absorbed water molecules and the second stage (in the region of 150–250 °C) has usually been assigned to the partial dehydroxylation of the LDH layer structure [39]. The major mass loss event is observed in the third stage and involves the decomposition of organic species and further dehydroxylation. This stage occurs earlier and more rapidly for the three-metal containing LDHs (AB, AC and AD) (around 270 °C), while a similar event covers a larger temperature range (from 270 to 420 °C) for the two-metal containing LDHs (AA and AE). A fourth event is observed in the temperature range 350–450 °C for the three-metal LDHs (AB, AC, AD), and above 450 °C for the two-metal LDHs (AA or AE), and can be attributed to further decomposition of the organic species that take place by several parallel and/or serial processes [40], such as dehydrogenation, thermal cracking to various hydrocarbons, decarboxylation and/or oxidation to CO_2, and graphitization. The final mass at 800 °C is found to be 26%, 30%, 32%, 33% and 36% for AA, AB, AC, AD and AE respectively. Throughout this work, these TGA residue at 800 °C percentages are used to determine the inorganic fraction of the LDHs, and the subsequent inorganic filler loadings of the polymer composites (the inorganic loadings investigated are 1%, 2% and 4% inorganic mass fraction of LDH).

3.3. Fire properties of the PP/oleate-LDH composites

The cone calorimeter is one of the most effective bench-scale methods for studying the flammability properties of materials. The heat release rate (HRR), and in particular the peak heat release rate (PHRR), has been found to be one of the most important parameters

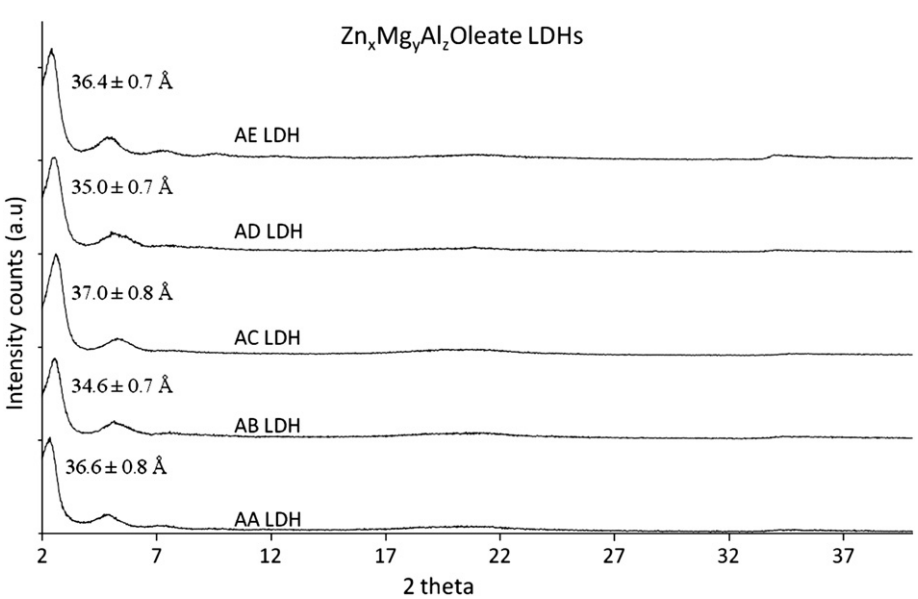

Fig. 1. XRD traces of the LDHs used in this work.

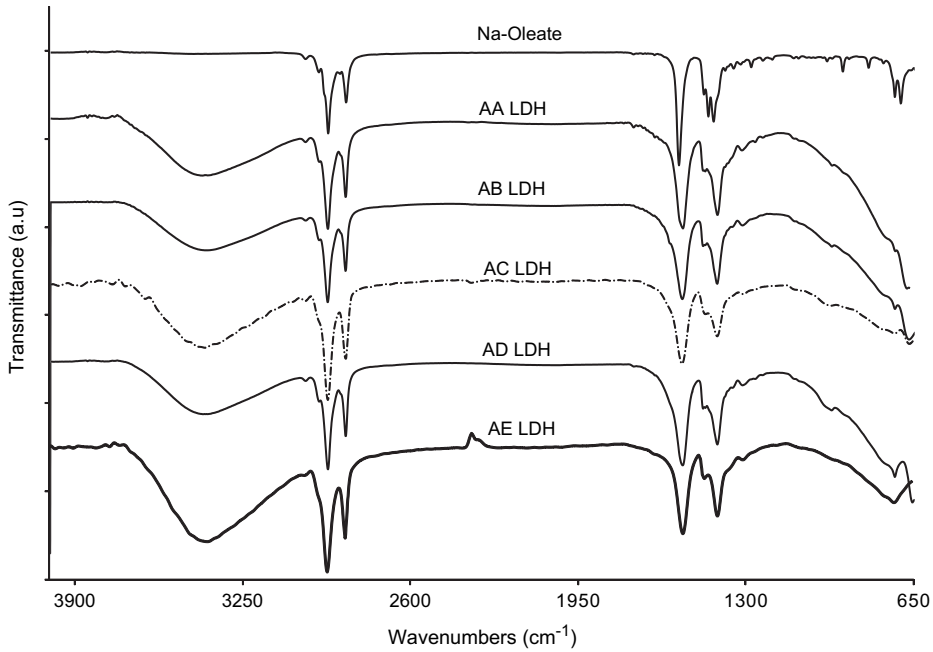

Fig. 2. ATR-IR of the five oleate-containing LDHs.

to evaluate fire safety [41–43], The reductions in the peak heat releases rates of the PP/oleate-LDHs relative to the pristine polymer during the combustion tests are shown in Fig. 4 and Table 2. At 1% LDH the five LDHs are ineffective as FR additives, as shown by an increase in the PHRR for all five systems (considering the ±10% error bars associated with cone calorimeter, there is no appreciable change in the PHRR at 1% LDH loading). At 2 wt.% LDH, the PHRR reductions are in the range 10–20%, and by doubling the LDH loading to 4 wt.% inorganic, the reductions still remain below 40% for the PP/LDH systems. At the highest loading studied in this work (4 wt.% LDH), the ternary LDHs perform better than the two-metal LDHs, but the reductions in PHRR obtained are lower than what has been reported for PP/MMT composites [32,44].

The low FR performance of the PP/LDH composite systems is consistent with a poor dispersion of the LDH nanofillers in the apolar PP matrix, which originates from the poor compatibility of the non-polar PP polymer with unmodified LDH, whose surface is defined by polar hydroxyl groups, and the interactions of the PP matrix with the oleate organic modification; in fact, poor dispersion of silicate layers at the nanometer level was previously reported for non-polar polymer matrices [28]. One of the strategies used to increase the compatibility between organically modified silicates, such as MMT and LDH, with non-polar polymers, like PP or PE, is to predisperse these fillers in similar polymers that are functionalized with polar groups (such as PP-*g*-MA, PE-*g*-MA, PE-*r*-VA, etc.) [22,24,45–47].

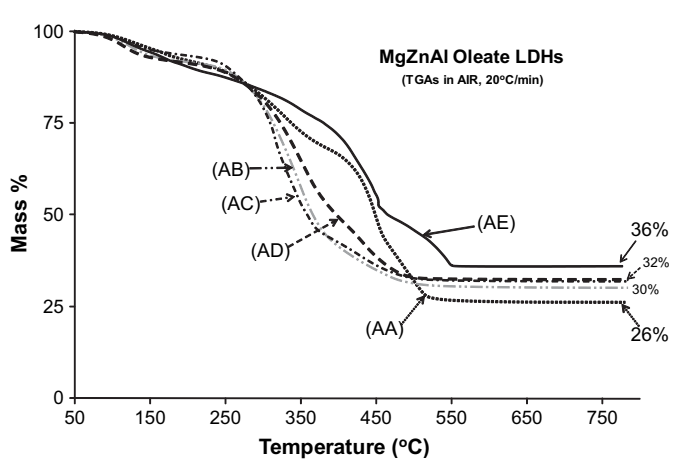

Fig. 3. TGA curves of oleate LDHs. The experiments were performed in an air environment, at 20 °C/min, in the temperature range 50–800 °C.

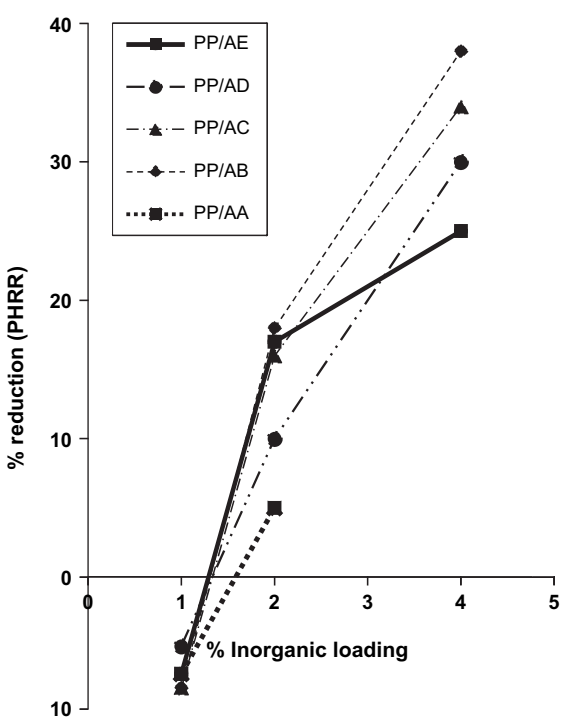

Fig. 4. The comparison of fire behavior of PP/oleate LDHs. % reduction in PHRR is plotted versus the % LDH inorganic loading.

Table 2
Cone summary results of PP modified with oleate-containing LDHs at 50 kW/m^2.

Formulation	PHRR (kW/m^2) (% reduction)	t_{PHRR} (s)	THR (MJ/m^2)	AMLR (g/s m^2)	t_{ign} (s)
PP	1849 ± 64 (NA)	116 ± 10	121 ± 4	30.5 ± 1.0	20 ± 2
PP/1% AE	1977 ± 54 (0)	107 ± 5	136 ± 2	29.6 ± 0.4	16 ± 0
PP/2% AE	1543 ± 154 (17)	91 ± 8	113 ± 3	25.9 ± 2.2	17 ± 2
PP/4% AE	1382 ± 41 (25)	98 ± 8	126 ± 0	23.6 ± 0.9	14 ± 1
PP/1% AD	1938 ± 23 (0)	111 ± 5	135 ± 1	29.1 ± 0.8	18 ± 1
PP/2% AD	1656 ± 150 (10)	106 ± 9	130 ± 1	26.4 ± 0.9	15 ± 1
PP/4% AD	1294 ± 71 (30)	84 ± 7	123 ± 3	22.3 ± 0.3	13 ± 1
PP/1% AC	2004 ± 129 (0)	116 ± 10	135 ± 2	29.3 ± 1.2	18 ± 1
PP/2% AC	1546 ± 59 (16)	94 ± 8	132 ± 1	25.3 ± 0.5	14 ± 1
PP/4% AC	1225 ± 80 (34)	73 ± 5	125 ± 1	20.3 ± 1.1	12 ± 2
PP/1% AB	1997 ± 136 (0)	56 ± 3	136 ± 2	28.9 ± 1.5	14 ± 1
PP/2% AB	1512 ± 28 (18)	110 ± 10	133 ± 1	25.7 ± 0.7	14 ± 1
PP/4% AB	1153 ± 15 (38)	117 ± 3	128 ± 1	21.6 ± 0.7	13 ± 1
PP/1% AA	1981 ± 126 (0)	113 ± 8	141 ± 1	28.4 ± 1.0	15 ± 1
PP/2% AA	1764 ± 99 (5)	109 ± 2	139 ± 1	27.4 ± 0.3	16 ± 1

Note: PHRR (kW/m^2) is the peak of heat release rate; (%red.) is the % reduction relative to the control sample; t_{PHRR} (s) is the time to PHRR; THR (MJ/m^2) is the total heat released; AMLR (g/s m^2); t_{ign} (s) is the time to ignition.

3.4. PP/PP-g-MA/LDH derivatives

To optimize the dispersion of LDH in PP, three different ratios of the non-polar matrix PP to the functionalized polymer (PP-*g*-MA) were evaluated: namely, PP:PP-*g*-MA ratios of 8:1; 4:1 and 1:1 were used, denoted hereafter as PP/PP-*g*-MA (*x*:*y*). Fig. 5 provides the HRR curves of PP:PP-*g*-MA (1:1)/LDH systems and the cone calorimetric data are summarized in Table 3. The addition of 1% LDH to the PP/PP-*g*-MA (1:1) system gives reductions in PHRR in the range 16–28%. When 4% of either LDH is added to PP/PP-*g*-MA (1:1) system, reductions in PHRR greater than 50% are obtained. In particular, PP/PP-*g*-MA (1:1)/4% AE gives a 68% reduction in PHRR relative to the pristine polymer. The pristine polymer and the composites have similar time to ignition, but the time to PHRR is lowered as the LDH loading is increased. In fact, once ignited, a carbonaceous layer is quickly formed on the surface of the polymeric sample and this layer probably plays a protecting role and reduces the heat transfer between the polymer and the heat source [41]. A correlation between the average mass loss rate and the reduction in PHRR for these systems at 4% LDH loading is also observed, which suggests that these materials function as condensed phase fire retardants.

The effect of varying the ratios of PP to PP-*g*-MA was also investigated. Tables 4 and 5 provide the cone calorimetric results of PP/PP-*g*-MA (8:1) and PP/PP-*g*-MA (4:1), respectively, modified with 1% and 4% (inorganic wt.%) of the five oleate-containing LDHs. In general, as the amount of PP-*g*-MA used is reduced, the reductions in PHRR at 4% LDH are also reduced. For example, PP/PP-*g*-MA (1:1) 4% AE gives a 68% reduction relative to the pristine polymers, while a 57% reduction is recorded when the ratio PP/PP-*g*-MA is 4:1 and this reduction is 51% when that ratio is 8:1. This is in concert with poorer filler dispersion as the amount of the functionalized PP copolymer is decreased, and is also in concert with lower enhancements in mechanical properties and in rheological manifestations of nanofiller dispersions [45]. The reductions in PHRR at 1% LDH loading are small throughout (below 30%), an indication of the ineffectiveness of the LDH as a fire retardant at such low filler loadings.

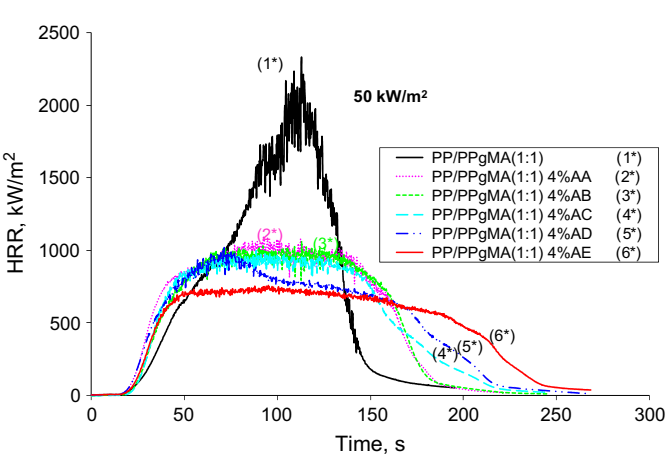

Fig. 5. Heat release rate (HRR) data for PP:PP-*g*-MA (1:1) and the corresponding PP/PP-*g*-MA/LDH systems.

Fig. 6 provides a comparison between the reductions in PHRR recorded at different ratios of PP/PP-*g*-MA. First, the variation in the LDH composition affects the reduction in PHRR. As the content of zinc is increased, from AA to AE, the resulting modified polymers have larger reductions in PHRR. A beneficial interaction between zinc-containing LDH modified with long organophilic surfactants, and a non-polar polymer, PE, was also observed in an earlier study [31]; both zinc aluminum and magnesium aluminum LDH modified with oleate anions were used as fillers for PE, and a 58% reduction in PHRR was recorded for PE/10 wt.% ZnAl composites, while PE/10 wt.% MgAl only gave a 28% reduction in PHRR relative to the pristine polymer [31].At the highest content of PP-*g*-MA in either system, the reductions in PHRR are above 50% which suggests that the compatibilizer is important in enhancing the fire retardancy properties of these systems. The best result in terms of the PHRR is obtained with the largest amount of the compatibilizer, PP-*g*-MA. When the amount of the LDHs is the largest, the PHRR values appear to be converging on a minimum value.

To explain the great enhancement in fire properties of the PP/oleate LDHs when the polymeric compatibilizer, PP-*g*-MA, is present, morphological studies of the samples before and after cone experiments were undertaken. Specifically, Figs. 7 and 8 provide the XRD traces of PP/PP-*g*-MA (*x*:*y*) at 1% and 4% loading of AA and AE. With either of the systems, a lower loading of LDH (1%) leads to the disappearance of the diffraction peaks, an indication that a disordered microcomposite (fillers remain in nanometer proximity but lose their parallel registry) or an exfoliated nanocomposite (fillers disperse in the polymer matrix, showing high interfiller separations) has been obtained. In the 4% AA LDH composites the first diffraction maxima are at comparable diffraction angles with the LDH fillers, and the diffraction intensities are still strong, a behavior typical of microcomposites where no

Table 3
Cone summary results of PP/PP-*g*-MA (1:1) modified with 5 oleate-containing LDHs at 50 kW/m^2.

Formulation	PHRR (kW/m^2) (% reduction)	t_{PHRR} (s)	THR (MJ/m^2)	VOS (l)	AMLR (g/s m^2)	t_{ign} (s)
PP/PP-*g*-MA (1:1)	2380 ± 334 (NA)	100 ± 5	140 ± 7	1703 ± 43	30.0 ± 0.8	17 ± 1
PP/PP-*g*-MA (1:1) 1% AA	1906 ± 141 (20)	98 ± 8	135 ± 5	1631 ± 88	25.6 ± 0.6	20 ± 1
PP/PP-*g*-MA (1:1) 1% AB	1715 ± 8 (28)	100 ± 4	134 ± 2	1515 ± 196	23.4 ± 5.9	17 ± 2
PP/PP-*g*-MA (1:1) 1% AC	1875 ± 94 (21)	115 ± 6	130 ± 9	1673 ± 127	27.2 ± 2.1	16 ± 1
PP/PP-*g*-MA (1:1) 1% AD	2008 ± 109 (16)	113 ± 8	135 ± 2	1694 ± 198	26.7 ± 1.9	15 ± 5
PP/PP-*g*-MA (1:1) 1% AE	1796 ± 130 (25)	115 ± 8	13 ± 3	1728 ± 98	26.8 ± 1.4	17 ± 2
PP/PP-*g*-MA (1:1) 4% AA	1137 ± 69 (52)	84 ± 8	129 ± 1	1288 ± 271	21.0 ± 0.6	16 ± 2
PP/PP-*g*-MA (1:1) 4% Ab	1025 ± 63 (57)	98 ± 23	124 ± 2	1715 ± 77	20.6 ± 1.2	17 ± 1
PP/PP-*g*-MA (1:1) 4% AC	992 ± 30 (58)	106 ± 18	125 ± 0	1638 ± 103	20.1 ± 0.3	14 ± 2
PP/PP-*g*-MA (1:1) 4% AD	997 ± 49 (58)	69 ± 2	126 ± 1	1449 ± 216	17.8 ± 0.5	16 ± 0
PP/PP-*g*-MA (1:1) 4% AE	757 ± 18 (68)	88 ± 9	125 ± 2	1461 ± 169	15.3 ± 0.7	16 ± 1

Note: PHRR (kW/m^2) is the peak of heat release rate; (%red.) is the % reduction relative to the control sample; t_{PHRR} (s) is the time to PHRR; THR (MJ/m^2) is the total heat released; VOS (l) is the volume of smoke; AMLR (g/s m^2); t_{ign} (s) is the time to ignition.

appreciable filler dispersion occurred. However, in the case of 4% AE (ZnAl-oleate LDH) composites, the diffractions are broader and less intense than those of the LDH fillers, a strong indication of disordering of the LDH layers in the polymer matrix. When the highest ratio of the PP-*g*-MA compatibilizer is used, for example in the PP/PP-*g*-MA (1:1)/4% AE, a small shift toward lower angles is observed, indicating some intercalation of polymer chains into the LDH gallery or, at least, some polymer-induced restructuring of the LDH intergallery material; the accompanying broadening of these diffraction peaks and the lower diffracted intensities, suggest that any possible intercalation is accompanied by some dispersion and disordering.

The dispersion of these LDHs into polymer matrices was further accessed by transmission electron microscopy (TEM). The composite morphology can be directly observed via bright field transmission electron microscopy (TEM). The TEM images at low magnification are used to determine the overall dispersion of the layered material in the polymer, while the higher magnification images provide more detail on the nanometer scale dispersion (e.g., intercalated or exfoliated morphologies). As good fire properties were typically obtained for the composites with the highest content of LDHs, TEM investigations focused on the dispersion of composites containing 4% LDH.

From the TEM images of PP/PP-*g*-MA (1:1)/4% AA (Fig. 9), the observed structures can be described as a mixed intercalated/exfoliated morphology with most of the LDH layers being well-dispersed and disordered. The LDH tactoids, with typical sizes 50–150 nm, are swollen by polymer. The PP/PP-*g*-MA (1:1)/4% AE composites also show a mixed intercalated/exfoliated structure with the LDH layers mostly well-dispersed. The LDH tactoids show much smaller sizes than the tactoids in the PP/PP-*g*-MA (1:1)/4% AA, and are typically 10–30 nm with very few larger ones (at 50–150 nm), while the larger scale agglomerates are very-highly swollen by polymer (PP and PP-*g*-MA). Comparing the PP/PP-*g*-MA (1:1)/4% AA and the PP/PP-*g*-MA (1:1)/4% AE morphologies, the filler dispersions at the nanometer scale is more-or-less the same, while at the micrometer scale the PP/PP-*g*-MA (1:1)/4% AE seems better dispersed than the PP/PP-*g*-MA (1:1)/4% AA. This last may be due to differences in the LDH layer sizes, with AE being substantially smaller than AA in lateral dimensions and, consequently, leading to an easier dispersion of the corresponding AE agglomerates in PP/PP-*g*-MA (1:1) [compared to the ones in the PP/PP-*g*-MA (1:1)/4% AA].

TEM images on a sample of PP/AE that contains a smaller content of PP-*g*-MA were also obtained and compared with the previous two samples with higher PP-*g*-MA content. The structure of PP/PP-*g*-MA (8:1)/4% AE is also a mixed intercalated/exfoliated structure, but this sample contains well-defined agglomerates, 200–500 nm sizes, and, within these, there are tactoids of LDH platelets that seem intercalated, separated by many disordered LDH layers between these tactoids. These disordered layers seem less dispersed, of higher density and with smaller layer to layer separations, than those in the PP/PP-*g*-MA (1:1)/4% AE. Comparing PP/PP-*g*-MA (8:1)/4% AE and PP/PP-*g*-MA (1:1)/4% AE, the dispersion of the system with more PP-*g*-MA seems slightly better both at the nanometer and at the micrometer scales, in concert with the dispersion obtained by much larger montmorillonite silicates pre-dispersed in PP-*g*-MA before dilution by unmodified PP [45]. Overall, the TEM studies reveal good dispersion, considering the high additive loadings investigated [4% AA = 15.4% MgAl-oleate (wt.%), while 4% AE = 11.1% ZnAl-oleate (wt.%)]. In previous work from these laboratories, the maximum amount of LDH that has been used is 10% [16–19,21].

A correlation between the filler dispersion and the corresponding reductions in PHRR emerges from these data: With more PP-*g*-MA present, the highest level studied in this work was PP:PP-*g*-MA of 1:1, reductions in PHRR greater than 50% are observed with either ZnAl-oleate (AE) or MgAl-oleate (AA), and fair to good

Table 4
Cone summary results of PP/PP-*g*-MA (8:1) modified with 5 oleate-containing LDHs at 50 kW/m^2.

Formulation	PHRR (kW/m^2) (% reduction)	t_{PHRR} (s)	THR (MJ/m^2)	VOS (l)	AMLR (g/s m^2)	t_{ign} (s)
PP/PP-*g*-MA (8:1)	1975 ± 85 (NA)	113 ± 6	125 ± 3	1387 ± 227	41.0 ± 9.5	26 ± 3
PP/PP-*g*-MA (8:1) 1% AA	1831 ± 65 (7)	128 ± 32	149 ± 17	1691 ± 222	25.6 ± 0.5	21 ± 1
PP/PP-*g*-MA (8:1) 1% AB	1838 ± 216 (7)	102 ± 5	135 ± 1	1624 ± 132	24.7 ± 5.3	23 ± 2
PP/PP-*g*-MA (8:1) 1% AC	1676 ± 39 (15)	89 ± 3	137 ± 1	1583 ± 127	26.8 ± 0.6	20 ± 2
PP/PP-*g*-MA (8:1) 1% AD	1833 ± 47 (7)	93 ± 5	136 ± 2	1752 ± 165	27.5 ± 0.3	19 ± 2
PP/PP-*g*-MA (8:1) 1% AE	1966 ± 16 (0)	91 ± 6	136 ± 3	1112 ± 238	28.4 ± 1.1	18 ± 1
PP/PP-*g*-MA (8:1) 4% AA	1274V185 (35)	110 ± 6	127 ± 0	1817 ± 236	17.6 ± 5.9	23 ± 2
PP/PP-*g*-MA (8:1) 4% Ab	1017 ± 33 (49)	48 ± 5	126 ± 1	1543 ± 189	19.6 ± 0.6	18 ± 1
PP/PP-*g*-MA (81) 4% AC	981 ± 35 (50)	84 ± 17	124 ± 1	1800 ± 57	19.9 ± 0.5	17 ± 0
PP/PP-*g*-MA (8:1) 4% AD	1061 ± 45 (46)	53 ± 4	126 ± 1	1701 ± 25	17.5 ± 0.0	15 ± 3
PP/PP-*g*-MA (8:1) 4% AE	965 ± 51 (51)	65 ± 4	126 ± 1	1581 ± 264	19.0 ± 0.2	17 ± 3

Note: PHRR (kW/m^2) is the peak of heat release rate; (%red.) is the % reduction relative to the control sample; t_{PHRR} (s) is the time to PHRR; THR (MJ/m^2) is the total heat released; VOS (l) is the volume of smoke; AMLR (g/s m^2); t_{ign} (s) is the time to ignition.

Table 5
Cone summary results of PP/PP-*g*-MA (4:1) modified with 5 oleate-containing LDHs at 50 kW/m^2.

Formulation	PHRR (kW/m^2) (% reduction)	t_{PHRR} (s)	THR (MJ/m^2)	VOS (l)	AMLR (g/s m^2)	t_{ign} (s)
PP/PP-*g*-MA (4:1)	1726 ± 183 (NA)	132 ± 11	133 ± 1	1480 ± 99	26.7 ± 1.0	23 ± 2
PP/PP-*g*-MA (4:1) 1% AA	1763 ± 32 (0)	108 ± 7	121 ± 2	1131 ± 682	27.4 ± 1.0	22 ± 0
PP/PP-*g*-MA (4:1) 1% AC	1795 ± 99 (0)	110 ± 5	131 ± 1	1525 ± 3	28.3 ± 1.4	19 ± 1
PP/PP-*g*-MA (4:1) 1% AE	1845 ± 95 (0)	104 ± 4	130 ± 2	1596 ± 133	26.6 ± 2.8	21 ± 0
PP/PP-*g*-MA (4:1) 4% AA	1283 ± 165 (26)	120 ± 1	125 ± 2	1787 ± 139	22.7 ± 0.3	20 ± 2
PP/PP-*g*-MA (4:1) 4% AC	897 ± 30 (48)	50 ± 3	121 ± 3	2066 ± 58	17.1 ± 1.3	16 ± 1
PP/PP-*g*-MA (4:1) 4% AE	750 ± 6 (57)	107 ± 17	122 ± 1	2295 ± 28	15.4 ± 0.5	18 ± 2

Note: PHRR (kW/m^2) is the peak of heat release rate; (%red.) is the % reduction relative to the control sample; t_{PHRR} (s) is the time to PHRR; THR (MJ/m^2) is the total heat released; VOS (l) is the volume of smoke; AMLR (g/s m^2); t_{ign} (s) is the time to ignition.

dispersion was observed for these systems. Restated, at the higher 50% content of PP-*g*-MA in the composite polymer matrix, the variation of the LDH intralayer metal composition, from zinc to magnesium, leads to minor differences in dispersion, which may explain the FR effectiveness of both additives in PP. The role of the PP-*g*-MA compatibilizer is important, considering the slightly better dispersion of PP/PP-*g*-MA (1:1)/4% AE relative to PP/PP-*g*-MA (8:1)/4% AE and the corresponding reductions in PHRR (68% versus 51%), it is likely that PP-*g*-MA facilitates more favorable interaction between the non-polar polymer matrices and the LDH layers.

3.5. Analysis of cone calorimeter residues

Figs. 10 and 11 provide photographs of the cone residues of PP/PP-*g*-MA (ratios 8:1 and 1:1, respectively) filled with 4% LDHs. In either series, it is observed that AE leads to a more compact char relative to the others; this zinc-rich LDH also leads to the highest reduction in PHRR relative to other LDHs at the same loading. The above observation suggests that the morphology of the char plays an important role in the magnitude of the reduction in PHRR. The mass of these solid residues corresponds to about 4% of the mass of the original sample, which is the expected mass based on TGA calculations of the inorganic content at 800 °C for either LDH.

Characterization of the cone residue was further performed by XRD to identify the different crystalline phases present in the cone residue. At either ratio of PP to PP-*g*-MA, the XRD traces before calcination indicate the formation of zinc oxide, but no aluminum-containing species. However, by calcining the char at 1000 °C for one day, the spinel $ZnAl_2O_4$ is indexed along with ZnO [48]. In a previous study, when the chars for a PMMA/LDH system modified with both zinc aluminum undecenoate LDH [16] and zinc aluminum oleate LDH [31] were calcined at 1000 °C, these same materials were formed. This should be expected as PMMA, PP or PE leaves no char when combusted, and consequently the cone residue are mostly residues of the organically modified LDH, which contain both divalent and trivalent anions. Similarly, when magnesium aluminum oleate is used to modified PP/PP-*g*-MA (ratios 1:1; 4:1 or 8:1), the XRD traces of the cone residues indicate the formation of MgO and the spinel, $MgAl_2O_4$. The XRD traces of these residues have been shown in previous publications [16,31].

3.6. Control experiments

To investigate further the origin of the efficacy of layered double hydroxides in cone calorimetry experiments, combinations of metal hydroxides, $Zn(OH)_2$ or $Mg(OH)_2$ and $Al(OH)_3$ (with or without sodium oleate) were melt blended with PP/PP-*g*-MA(ratios 1:1; 4:1 and 8:1). The amounts of the three metal hydroxides was chosen to correspond to the same metal ratios and the same metal loadings as those in the LDH composites at 4% loading; subsequently, the fire retardant properties of the resulting composites are compared to those of the corresponding LDH systems.

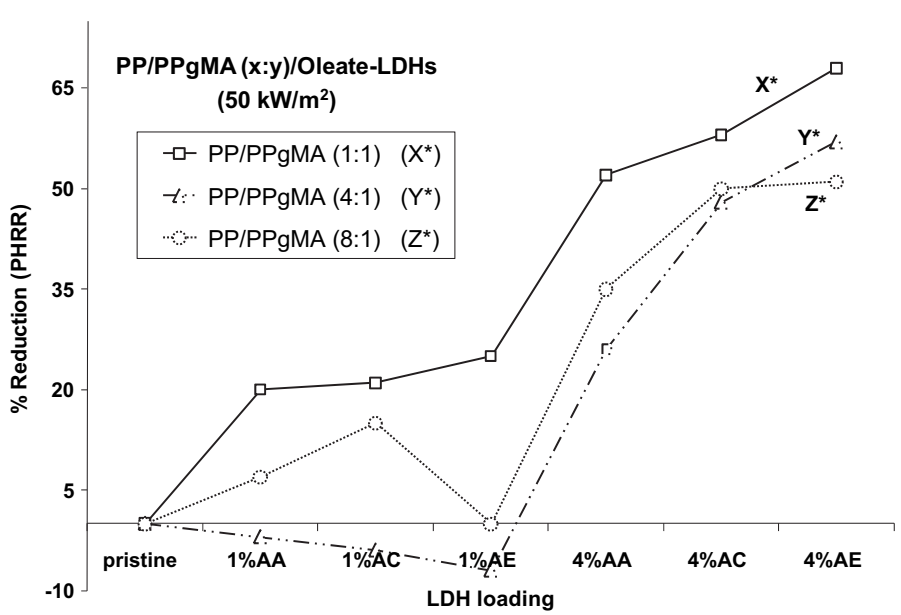

Fig. 6. The effect of PP/PP-*g*-MA ratio on the combustion their modified LDH systems; the reductions in PHRR of the composites relative to the prestine polymers are plotted against the LDH loading.

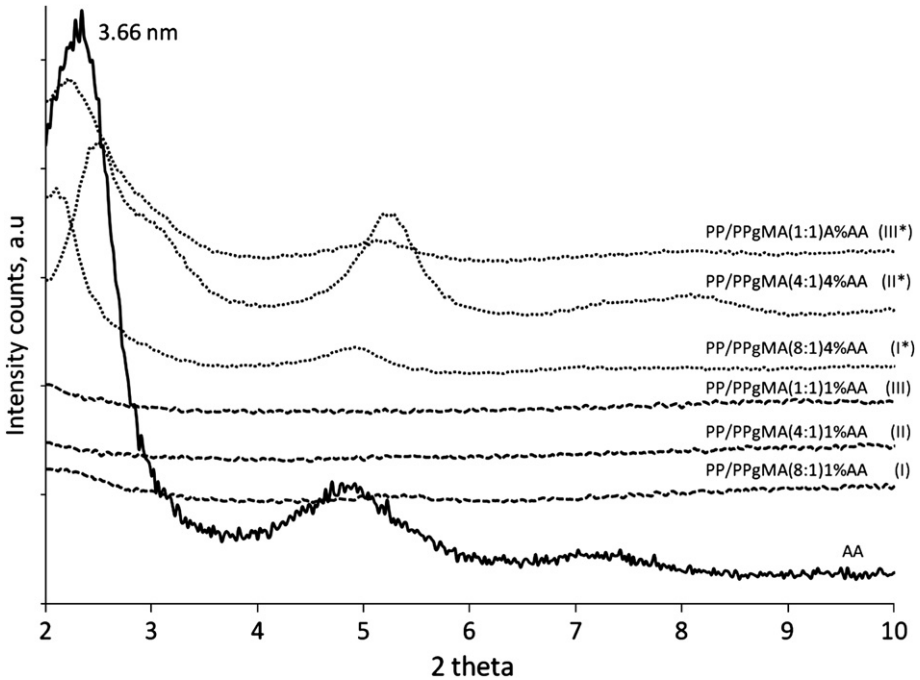

Fig. 7. XRD traces of PP/PP-*g*-MA (*x*:*y*)/1% AA (I, II, III) and PP/PP-*g*-MA (*x*:*y*) 4% AA (I*, II*, III*).

Table 6 provides the cone results for PP/PP-*g*-MA (1:1) at 50 kW/m^2 filled with mixtures of commercial metal hydroxides. The reductions in PHRR, relative to pristine polymer, range between 10 and 22%, while all five oleate-containing LDHs gave more than 50% reductions in PHRR with the same polymers. This superior FR performance of LDH relative to the 'equivalent' combinations of commercial metal hydroxides, is further exemplified by the combinations of metal hydroxides with or without oleate anions. As observed in Table 6, the addition of the organic molecules to the metal hydroxides, reproducing the same metal and organic contents as either ZnAl LDH (AE) or MgAl LDH (AA), leads to low reductions in PHRR (less than 20%). All the above suggest that the LDH offers superior flame protection to PP relative to the 'equivalent' combinations of metal hydroxides, *i.e.*, combinations that have the same metal and organic contents as the corresponding LDHs.

Contrary to the polymer/LDH composites, the char residues of the PP filled by the combinations of the metal hydroxides showed only tiny particles left on the aluminum foil after combustion; the mass of these residues, however, corresponds to the expected inorganic based on the amount of metal hydroxides used (∼4%).

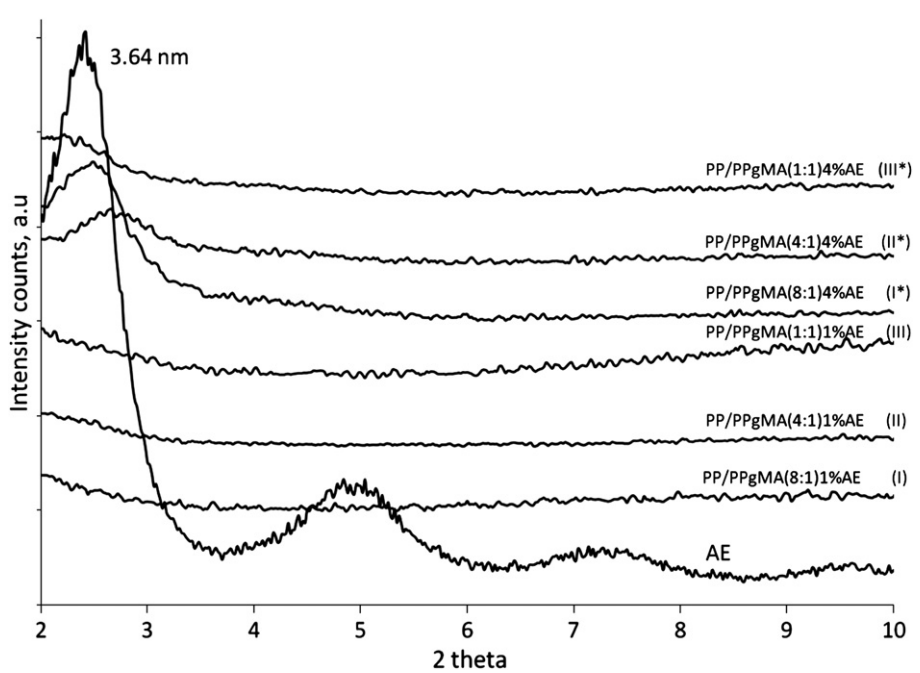

Fig. 8. XRD traces of ZnAl-oleate LDH (AE) and PP/PP-*g*-MA (*x*:*y*)/1% AE (I, II, III) and PP/PP-*g*-MA (*x*:*y*) 4% AE (I*, II*, III*).

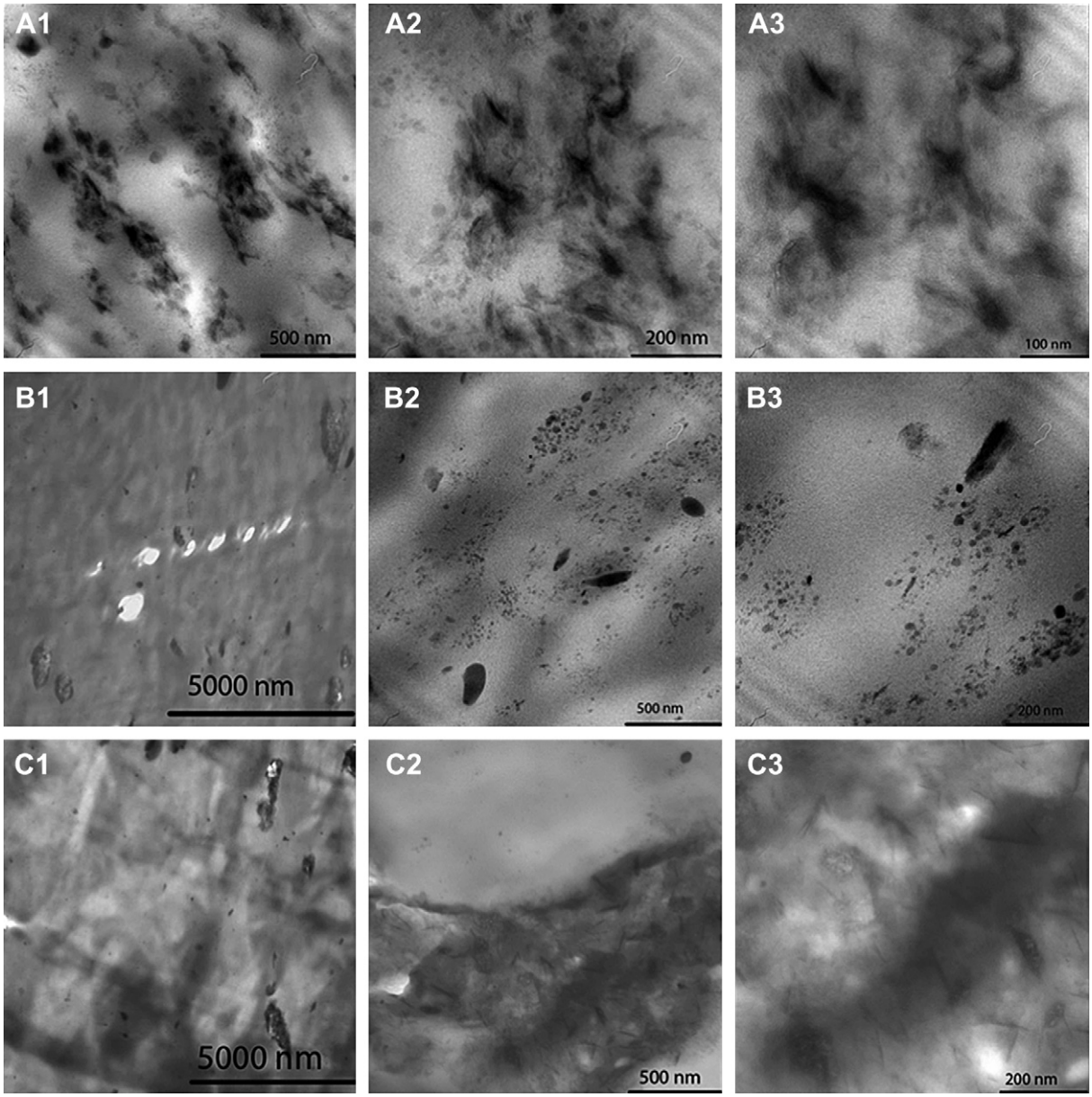

Fig. 9. The TEM images of PP:PP-*g*-MA (1:1) 4% MgAl-oleate (A1, A2, A3), PP:PP-*g*-MA (1:1) 4% ZnAl-oleate (B1, B2, B3) and PP:PP-*g*-MA (8:1) 4% ZnAl-oleate (C1, C2, C3) at different magnifications.

This behavior strongly suggests that the efficacy of LDHs in lowering the PHRR of the polymer composites is probably due to the formation of a relatively compact inorganic layer on the surface of the polymeric sample upon exposure to flame, rather than due to the mass of the residue.

The cone residues of PP/metal hydroxide systems were also characterized by XRD, and the different phases present were identified [48]. As in the case of organically modified LDHs (ZnAl and MgAl), the same crystal phases ZnO/$ZnAl_2O_4$ and MgO/$MgAl_2O_4$ were identified in these char residues after calcination. These results suggest however that the formation of spinel from various mixtures of metal hydroxides is both temperature and time dependent. For example, the XRD of the residues from the combinations of metal hydroxides corresponding to the same metal content as the AE LDH, do not show the spinel phase when calcined at 1000 °C overnight. To investigate if these metal hydroxides will also eventually lead to both the spinel, $ZnAl_2O_4$, and ZnO, the chars were calcined as follows: part of the char is calcined to 700 °C for 10 h, and the other part is calcined firstly at 700 °C (10 h) and subsequently at 1000 °C (10 h). Both the composition with and without organic oleate anions were evaluated. As shown in Fig. 12, at 700 °C, ZnO is the dominant phase for both types of char, but in the char from the sample prepared with oleate anions, another minor phase is identified (indicated by ■). This minor phase, possibly Al_2O_3, is also observed when PP/PP-*g*-MA (1:1) with the metal hydroxide composition corresponding to AE is calcined at 1000 °C for 12 h. The diffractions of this phase disappear when the 700 °C char is further calcined at 1000 °C for another 10 h, where only zinc oxide and the spinel, $ZnAl_2O_4$, are indexed. The above XRD observations confirm that the crystal phase at room temperature for either system is ZnO and, when these materials are heated, they all eventually lead to the formation of both ZnO and $ZnAl_2O_4$, as was observed with zinc aluminum LDHs. The utility of LDHs in the synthesis of $M^{II}M^{III}{}_2O_4$ spinels is apparent, considering the longer

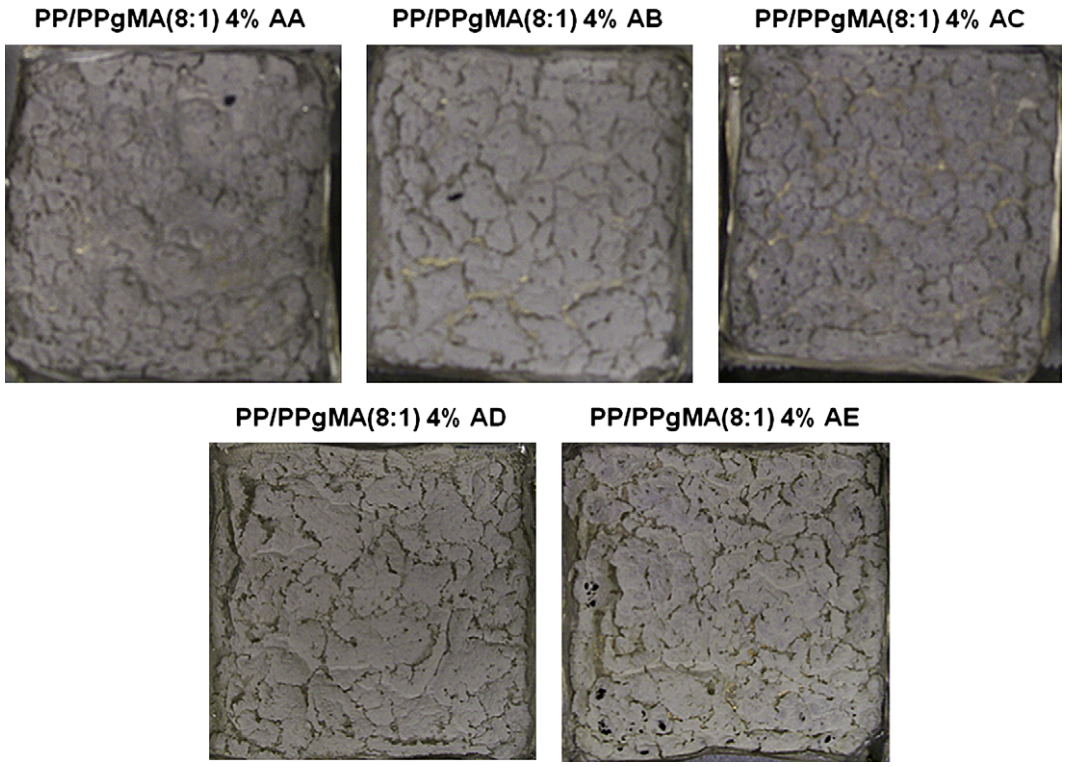

Fig. 10. Pictures of the cone residues of PP/PP-*g*-MA (8:1) modified with oleate-containing LDHs. *Note*: the % mass of solid residue relative to initial cone plaque is: 4.2% [PP/PP-*g*-MA (8:1) 4% AA]; 4.0% [PP/PP-*g*-MA (8:1) 4% AB]; 4.7% [PP/PP-*g*-MA (8:1) 4% AC]; 4.3% [PP/PP-*g*-MA (8:1) 4% AD]; 4.3% [PP/PP-*g*-MA (8:1) 4% AE]. The reported % mass is an average of 3 determinations, calculated based on 30 g of the initial cone plaque before burning.

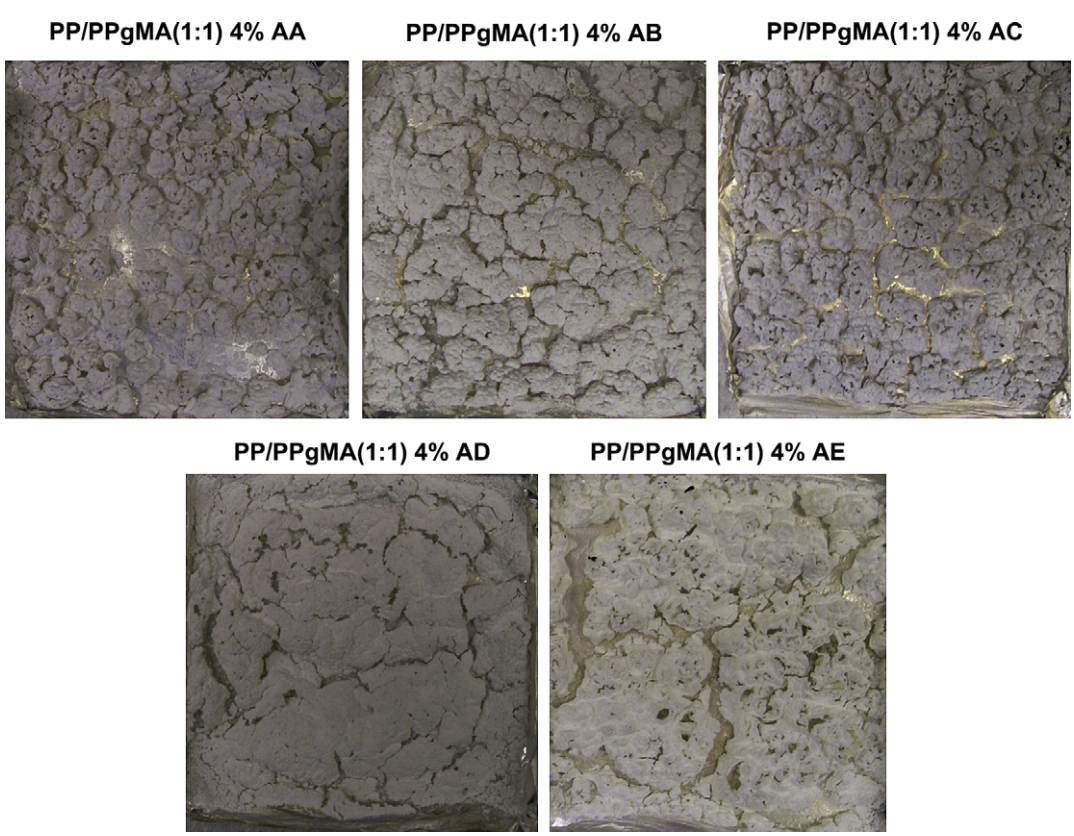

Fig. 11. Pictures of the cone residues of PP/PP-*g*-MA (1:1) modified with oleate-containing LDHs. *Note*: the % mass of solid residue relative to initial cone plaque is: 4.2% [PP/PP-*g*-MA (1:1) 4% AA]; 4.0% [PP/PP-*g*-MA (1:1) 4% AB]; 4.7% [PP/PP-*g*-MA (1:1) 4% AC]; 4.3% [PP/PP-*g*-MA (1:1) 4% AD]; 4.3% [PP/PP-*g*-MA (1:1) 4% AE]. The reported % mass is an average of 3 determinations, calculated based on 30 g of the initial cone plaque before burning.

Table 6
Cone summary results of PP/PP-*g*-MA (1:1) modified with metal hydroxides $Zn(OH)_2$ or $Mg(OH)_2$ and $Al(OH)_3$ simulating the 5 oleate-containing LDHs at 50 kW/m^2.

Formulation	PHRR (kW/m^2) (% reduction)	t_{PHHR} (s)	AMLR (g/s m^2)	t_{ign} (s)
PP/PP-*g*-MA (1:1)	1968 ± 309 (NA)	107 ± 4	30.0 ± 0.6	20 ± 0.5
PP/PP-*g*-MA + MOHs [AA]	1778 ± 12 (10)	116 ± 15	22.8 ± 5.9	18 ± 1.2
PP/PP-*g*-MA + MOHs [AA] + Oleate	1694 ± 306 (14)	122 ± 5	25.2 ± 2.3	25 ± 1.5
PP/PP-*g*-MA + MOHs [AB] + Oleate	1532 ± 115 (22)	117 ± 5	22.9 ± 4.9	20 ± 1.7
PP/PP-*g*-MA + MOHs [AC] + Oleate	1710 ± 251 (13)	111 ± 5	25.7 ± 0.6	19 ± 1.0
PP/PP-*g*-MA + MOHs [AD] + Oleate	1770 ± 190 (10)	114 ± 9	25.3 ± 0.5	20 ± 2.6
PP/PP-*g*-MA + MOHs [AE] + Oleate	1640 ± 200 (17)	120 ± 6	24.5 ± 0.2	21 ± 2.0
PP/PP-*g*-MA + MOHs [AE]	1597 ± 179 (19)	109 ± 9	24.3 ± 1.9	18 ± 1.6

Note: MOHs [LDH] is the combination of $Zn(OH)_2$ and/or $Mg(OH)_2$ with $Al(OH)_3$ to simulate the target LDH at 4% inorganic loading.

time required to make these same materials from 'equivalent' combinations of metal oxides with the same polymers. Spinels continue to attract a great deal of interest because of their many applications [49,50].

3.7. Thermogravimetric analysis

The thermal stability of PP/PP-*g*-MA at various ratios of PP to PP-*g*-MA and their corresponding LDH composites were also evaluated by TGA experiments, in air, at 20 °C/min, from 50 to 800 °C. Any given mass loss can be used as reference when comparing different materials, but most frequently the onset temperature (temperature at 10% mass loss, or $T_{0.1}$) and the midpoint temperature of degradation (temperature at 50% mass loss, or $T_{0.5}$) are used to evaluate the thermal properties of materials.

From Table 7, at any ratio of PP to PP-*g*-MA and for all LDH fillers, an improvement in the onset temperature and in the midpoint temperature is observed. This behavior indicates that organophilic

Table 7
TGA summary results of PP/PP-*g*-MA/oleate LDHs.

Material	$T_{0.1}$ (°C)	ΔT	$T_{0.5}$ (°C)	ΔT	% Char at 600 °C
PP/PP-*g*-MA (8:1) control	318	NA	385	NA	0
PP/PP-*g*-MA (8:1) 4% AA	381	63	436	51	4
PP/PP-*g*-MA (8:1) 4% AB	363	45	419	34	4
PP/PP-*g*-MA (8:1) 4% AC	355	37	414	29	4
PP/PP-*g*-MA (8:1) 4% AD	350	32	425	40	4
PP/PP-*g*-MA (8:1) 4% AE	355	37	416	31	4
PP/PP-*g*-MA (4:1) control	319	NA	381	NA	0
PP/PP-*g*-MA (4:1) 4% AA	365	46	425	44	4
PP/PP-*g*-MA (4:1) 4% AC	354	35	418	37	4
PP/PP-*g*-MA (4:1) 4% AE	348	29	416	35	4
PP/PP-*g*-MA (1:1) control	324	NA	398	NA	0
PP/PP-*g*-MA (1:1) 4% AA	363	39	425	27	4
PP/PP-*g*-MA (1:1) 4% AB	355	31	428	30	4
PP/PP-*g*-MA (1:1) 4% AC	349	25	421	23	3
PP/PP-*g*-MA (1:1) 4% AD	349	25	419	21	3
PP/PP-*g*-MA (1:1) 4% AE	353	29	421	23	4

Note: $T_{0.1}$ – temperature of 10% mass loss; $T_{0.5}$ – temperature of 50% mass loss; ΔT – difference between virgin polymer and its composite.

LDHs have great potential for polymer reinforcement; the presence of the hydrotalcite-like lamellae produces a barrier to oxygen diffusion into the heated polymer due to the accumulation of the oxides produced by thermal degradation of the material on the surface of the volatizing polymer [51]. PP/PP-*g*-MA (1:1)/4% AA shows the greatest improvement, increasing the $T_{0.1}$ by 63 °C and the $T_{0.5}$ by 53 °C, compared to PP/PP-*g*-MA (1:1). The magnesium content in the LDH affects the thermal stability in the PP/PP-*g*-MA/LDH systems; at all ratios of PP/PP-*g*-MA, the best improvements are noted with MgAl LDH (AA) and the smallest improvements are seen with ZnAl LDH (AE). This finding is in contrast with the cone results, where the reduction in PHRR is greatest for the zinc-rich systems. Improvement in both fire and thermal properties are usually desired, and a system that performs well both in TGA and cone experiments is targeted. There is no evidence of correlation between the two properties in the above data. The fraction of non-volatiles that remains at 600 °C, denoted as char in the table, is about 4% for all composites. This suggests that little or no organic

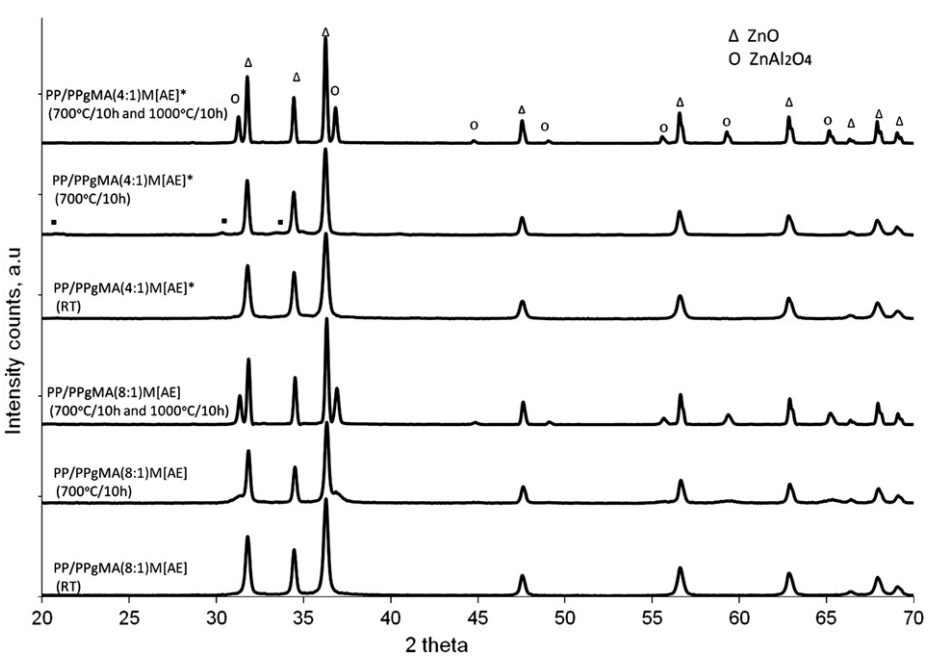

Fig. 12. XRD traces of PP/PP-*g*-MA (*x*:*y*)/MOHs [AE] (cone chars) at both room temperature (RT) and calcined to 700 °C (10 h) and both, 700 °C (10 h), then 1000 °C (10 h). MOHs [AE]: $Zn(OH)_2$ + $Al(OH)_3$, as calculated from elemental analysis, equivalent to 4% AE in PP/PP-*g*-MA (*x*:*y*); and (*) denotes samples containing oleate anions (from Na-oleate) as calculated from elemental analysis of AE. *Note*: (△ZnO, PDF 36-1451; ○$ZnAl_2O_4$, PDF 5-0671, and ■ denotes another phase, possibly Al_3O_4).

Table 8
TGA summary results of PP/PP-*g*-MA (1:1), Na-oleate (commercial) and the combinations of metal nitrates and Na-oleate simulating AB, AC, AD, AE and AA LDHs.

Material	$T_{0.1}$ (°C)	$T_{0.5}$ (°C)	Char
PP/PP-*g*-MA (1:1)	324	398	0
Na-Oleate	421	495	16
PP/PP-*g*-MA + MOHs [AA][a]	317	388	3
PP/PP-*g*-MA + MOHs [AB] + Na-oleate	374	434	5
PP/PP-*g*-MA + MOHs [AC] + Na-oleate	353	428	6
PP/PP-*g*-MA + MOHs [AD] + Na-oleate	357	428	4
PP/PP-*g*-MA + MOHs [AE] + Na-oleate	354	423	5
PP/PP-*g*-MA + MOHs [AB][a]	333	400	5

Note: $T_{0.1}$ – temperature of 10% mass loss; $T_{0.5}$ – temperature of 50% mass loss; $\triangle T$ – difference between virgin polymer and its composite.
[a] These samples do not contain Na-oleate.

material (polymer or LDH anion) is left-over after the TGA experiment, since 4% char is the amount expected from the LDH inorganic alone.

The thermal properties of PP/PP-*g*-MA (1:1) modified with combinations of commercial metal hydroxides and sodium oleate (as before, used at amounts corresponding to the same metal and anion contents as the LDHs) were also evaluated in TGA experiments (air environment, 20 °C/min, results shown in Table 8). Sodium oleate is stable enough to survive the processing conditions, only 10% of the salt is lost at 400 °C, and it forms 16% char at 600 °C (this amount is twice the amount of solid residue that would be obtained if all organic content is lost in TGA experiment and the char formed contains only the sodium content of the salt, *i.e.*, 7%). The combination of Na-oleate with the commercial metal hydroxide 'equivalent' to 4% LDH enhances the thermal stability of the polymers relative to pristine polymer. The addition of Na-oleate improves the thermal stability compared to systems without Na-oleate, which can be expected as the salt alone is more thermally stable than PP:PP-*g*-MA under similar conditions. At both 10% and 50% mass loss, the following trend is noted: as more magnesium is added to a particular combination, the more thermally stable it becomes. These results suggest that the trend observed with LDH is due to the metals, magnesium versus zinc.

4. Conclusion

Five oleate-containing LDHs of the general formula $Zn_xMg_yAl(OH)_6(oleate)]\cdot nH_2O$ with $x + y = 2$ were successfully prepared by the coprecipitation method. ATR-IR and XRD studies show that oleate anions are present in the materials and that these materials are layered with large interlayer spaces of 3.5–3.7 nm. Oleate-containing LDHs are thermally stable to above 250 °C which make them good candidate for the preparation of PP and PP-*g*-MA composites, melt-processed at 180 °C. TGA experiments of the PP composites indicate that the magnesium content in the LDH, or in equivalent combinations of commercial metal hydroxides, correlates well with the thermal stability of the PP/LDH composites: systems with more magnesium show enhanced thermal stability relative to the respective ones with zinc-containing additives. Straightforward addition of oleate-containing LDHs is not effective at lowering the PHRR of PP systems, but with the addition of a PP-*g*-MA compatibilizer to improve the filler dispersion, results in PP/PP-*g*-MA/4% LDHs which show large reductions in PHRR (up to 68% reduction in PHRR for PP/PP-*g*-MA (1:1) 4% AE). The large reductions in PHRR were correlated to the morphology of the composites, where good nanometer dispersion were observed by TEM. Also, the cone residues (chars) reveal a more compact but light char, while the combination of metal hydroxides form small particulate chars and then give poor fire behavior. XRD traces of the cone residues of PP/PP-*g*-MA systems modified with ZnAl-oleate or combinations of $Zn(OH)_2$ and $Al(OH)_3$ with or without Na-oleate reveal that ZnO is the only crystalline phase, and both ZnO and $ZnAl_2O_4$ are identified when the char is calcined at high temperatures; the time required to form both ZnO and the spinel depends on the additive used with the LDH-containing systems requiring above 10 h at 1000 °C but the combination of $Zn(OH)_2$ with $Al(OH)_3$ with or without Na-oleate required more time, which highlight the advantage of using LDH as precursors for spinels of the type $M^{II}M^{III}{}_2O_4$.

References

[1] Theng BKG. Formation and properties of clay–polymer complexes. Elsevier; 1979;
Krishnamoorti R, Vaia RA, editors. Polymer nanocomposites. ACS; 2001;
Pinnavaia TJ, Beall GW, editors. Polymer–clay nanocomposites. Wiley; 2001;
Mai Y, Yu Z, editors. Polymer nanocomposites. Woodhead Publishing; 2006;
Morgan AB, Wilkie CA, editors. Flame retardant polymer nanocomposites. Wiley; 2007.
[2] Zhang J, Manias E, Wilkie CA. J Nanosci Nanotechnol 2008;8:1597;
Morgan AB. Polym Adv Technol 2006;17:206;
Usuki A, Hasegawa N, Kato M. Adv Polym Sci 2005;179:135;
Ray SS, Okamoto M. Prog Polym Sci 2003;28:1539;
Alexandre M, Dubois P. Mater Sci Eng R 2000;28:1;
Giannelis EP, Krishnamoorti R, Manias E. Adv Polym Sci 1999;138:107;
LeBaron PC, Wang Z, Pinnavaia TJ. Appl Clay Sci 1999;15:11;
Giannelis EP. Adv Mater 1996;8:29;
Komarneni S. J Mater Chem 1992;2:1219.
[3] Leroux F, Besse JP. Chem Mater 2001;13:3507;
De Roy A, Forano C, El Malki K, Besse J-P. In: Occeli L, Robson H, editors. Synthesis of microporous materials, vol. 2. New York: Van Nostrand Rheinhold; 1992. p. 108;
Solin SA, Hines D, Yun SK, Pinnavaia TJ, Thorpe MF. J Non-Cryst Solids 1995;185:212.
[4] Lucrédio AF, Assaf EM. J Power Sources 2006;159:667.
[5] Kuzawa K, Jung YJ, Kiso Y, Yamada T, Nagai M, Lee TG. Chemosphere 2006;62:45.
[6] Yang WS, Kim Y, Liu PKT, Sahimi M, Tsotsis TT. Chem Eng Sci 2002;57:2945.
[7] Kim D, Lee JS, Barry CMF, Mead JL. Polym Eng Sci 2007;47:2049.
[8] Chen W, Qu B. Chem Mater 2003;15:3208.
[9] Li B, hu Y, Liu J, Chen Z, Fan W. Colloid Polym Sci 2003;281:998.
[10] Chen W, Feng L, Qu B. Chem Mater 2004;16:368.
[11] Hsueh HB, Chen CY. Polymer 2003;44:1151.
[12] Qiu L, Chen W, Qu B. Polym Degrad Stab 2005;87:433.
[13] TaviotGueho C, Leroux F. Struct Bonding 2006;119:121.
[14] Cho MS, Shin B, Choi SD, Lee Y, Song K. Electrochim Acta 2004;50:331.
[15] Cho MS, Shin B, Do Nam J, Lee Y, Song K. Polym Int 2004;53:1523.
[16] Manzi-Nshuti C, Hossenlopp JM, Wilkie CA. J Mater Chem 2008;18:3091.
[17] Nyambo C, Songtipya P, Manias E, Jimenez-Gasco MM, Wilkie CA. J Mater Chem 2008;18:4827–38.
[18] Wang LJ, Su S, Wilkie CA. Polym Degrad Stab 2009;94:770.
[19] Manzi-Nshuti C, Wang D, Hossenlopp JM, Wilkie CA. Polym Degrad Stab 2009;94:705.
[20] Babrauskas. V, Peacock RD. Fire Saf J 1992;18:255.
[21] Nyambo C, Wang D, Wilkie CA. Polym Adv Technol 2009;20:332.
[22] Tidjani M, Wilkie CA. Polym Degrad Stab 2001;74:33.
[23] Bartholmai M, Schartel B. Polym Adv Technol 2004;15:355.
[24] Manias E, Touny A, Wu L, Strawhecker K, Lu B, Chung TC. Chem Mater 2001;13:3516.
[25] Yuan Q, Misra RDK. Polymer 2006;47:4421.
[26] Chrissopoulou K, Altintzi I, Andrianaki I, Shemesh R, Retsos H, Giannelis EP, et al. J Polym Sci Part B Polym Phys 2008;46:2683–95.
[27] Wang ZM, Nakajima H, Manias E, Chung TC. Macromolecules 2003;36:8919.
[28] Wang DY, Wilkie CA. Polym Degrad Stab 2003;80:171.
[29] Alexander M, Beyer G, Henrist C, Cloots R, Rulmont A, Jerome R, et al. Chem Mater 2001;13:3830.
[30] Hu Y, Tang Y, Song L. Polym Adv Technol 2006;17:235.
[31] Manzi-Nshuti C, Songtipya P, Manias E, Jimenez-Gasco MM, Hossenlopp JM, Wilkie CA. Polymer 2009:3564–74.
[32] Gilman JW, Kashiwagi T, Nyden M, Brown JET, Jackson CL, Lomakin S, et al. In: Al-Malaika S, Golovoy A, Wilkie CA, editors. Chemistry and technology of polymer additives. Oxford: Blackwell Scientific; 1999. p. 249–65.
[33] Jiao CM, Wang ZZ, Chen ZL, Hu Y. J Appl Polym Sci 2008;107:2626.
[34] Lin Y, Wang J, Evans DG, Li D. J Phys Chem Solids 2006;67:998.
[35] Wang GA, Wang CC, Chen CY. Polymer 2005;46:5065.
[36] Costantino U, Marmottini F, Nocchetti M, Vivani R. Eur J Inorg Chem 1998;10:1439.
[37] Xu ZP, Braterman PS, Yu K, Xu H, Wang Y, Brinker CJ. Chem Mater 2004;16:2750.
[38] Simons WW, editor. The Sadtler handbook of infrared spectra. Philadelphia, PA: Sadtler Research Laboratories, Inc.; 1978. pp. 26, 710, and 741.

[39] Xu ZP, Braterman PS, Yu K, Xu H, Wang Y, Brinker CJ. Chem Mater 2004;16:2750.
[40] Xu ZP, Zeng HC. J Phys Chem B 2000;104:10206.
[41] Gilman JW, Jackson CL, Morgan AB, Harris R, Manias E, Giannelis EP, et al. Chem Mater 2000;12:1866.
[42] Tang Y, Hu Y, Song L, Zong RW, Gui Z, Chen ZY, et al. Polym Degrad Stab 2003;82:127.
[43] Zanetti M, Kashiwagi T, Falqui L, Camino G. Chem Mater 2002;14:881.
[44] Su S, Jiang DD, Wilkie CA. Polym Degrad Stab 2004;83:321.
[45] Xu L, Nakajima H, Manias E, Krishnamoorti R. Tailored nanocomposites of polypropylene with layered silicates. Macromolecules 2009;42:3795–803.
[46] Manias E, Zhang J, Huh JY, Manokruang K, Songtipya P, Jimenez-Gasco MM. Macrom Rapid Commun 2009;30:17.
[47] Zhang J, Manias E, Polizos G, Huh JY, Ophir A, Songtipya P, et al. J Adhes Sci Technol 2009;23:709.
[48] Powder diffraction file alphabetical indexes, inorganic phases. Swarthmore, PA: JCPDS, International Centre for Diffraction Data; 1999.
[49] Pileni MP. Adv Funct Mater 2001;11:323.
[50] Yu SH, Yoshimura M. Adv Funct Mater 2002;12:9.
[51] Camino G, Maffezzoli A, Braglia M, De Lazzaro M, Zammarano M. Polym Degrad Stab 2001;74:457.